Well-Defined, Model Long Chain Branched Polyethylene. 2. Melt Rheological Behavior

D. J. Lohse,* S. T. Milner, L. J. Fetters,† and M. Xenidou

ExxonMobil Research & Engineering Co., Annandale, New Jersey 08801

N. Hadjichristidis

Department of Chemistry, University of Athens, Greece

R. A. Mendelson,‡ C. A. García-Franco, and M. K. Lyon

ExxonMobil Chemical Company, Baytown, Texas 77520-2101

Received October 9, 2001

ABSTRACT: In this paper, we examine the melt rheology of well-defined, model polymers where the long chain branching (LCB) is precisely known from the synthesis. All of these are made by the hydrogenation of polybutadiene, but they vary greatly in the level and type of LCB present. We find that all polymers that have LCB show a greater degree of shear thinning than linear chains. This applies both to those with a single branch (stars) and also to those with multiple branches per chain (such as combs). However, only molecules with multiple branches induce extensional thickening in a sample. Only a small amount of these comblike molecules, on the order of 5%, are needed to show this effect. We also show here how a new method of treating the shear data, the so-called Van Gurp−Palmen analysis, can give a more easily interpreted form of the results that can reveal the length and amount of branches in a sample. The insights generated from this work show the importance of access to well-defined polymers with several kinds of branching architecture for the development of a deeper understanding of polymer rheology.

Introduction

The value of long chain branching (LCB) in polyethylene (PE) has long been known. Even though most of the physical properties (e.g., toughness) of low density PE (LDPE) are generally inferior to those of linear low-density PE (LLDPE), the former still has a large share of the market due to its greater processability. The rheological behavior that leads to this enhanced processability of LDPE is attributed to the presence of long branches.[1] By "long" we mean here a branch with a molecular weight at least greater than the entanglement molecular weight, M_e, which is around 1 kg/mol for PE[2].

The advent of metallocene and other "single-site" catalysts has renewed interest in LCB for PE and its effects on rheology. There are now many reports of polyethylenes (homopolymers and copolymers) made by such catalysts that clearly exhibit many of the features of long branches.[3,4] There is evidence for a difference in how the sizes of these polyethylene chains depend on molecular weight compared to linear ones, which can only be due to high levels of branching.[5−7] Spectroscopic data cannot provide direct proof for the presence of branches as long as those of interest here, but do lend indirect support to the formation of long branches.[8] Most importantly, the rheological behavior of these polymers is highly consistent with the presence of LCB, and they do show greater ease of processing than linear PE.[1,9−11] The mechanisms for the formation of LCB by metallocene and other single-site catalysts are still not completely clear, and probably differ among the various catalysts and polymerization conditions. It is clear, however, that the method of LCB formation is different from that in free radical ethylene polymerization, which means that the nature of the LCB is different as well.

Defining the nature of LCB in a particular polymer sample is both a difficult and complicated task. It is difficult because of the low level of branching present in the polymers of most interest. Since the branches (and the spacing between the branch points on the backbone) need to have a molecular weight greater than the entanglement molecular weight of polyethylene, which is about 1 kg/mol, the number of carbons serving as the node of a long branch can be no more than one in a hundred, and is generally much less. Often the signal from such branch points can be masked by a large degree of short branching, such as that due to the incorporation of α-olefins like 1-butene or 1-octene.[8] This makes spectroscopic identification of LCB highly problematic.

The characterization of LCB is also highly complicated. Many variables are needed to completely specify the nature of LCB in a polymer. The first is the functionality of the branch point—trifunctional, tetrafunctional, or greater. Second, one also has to specify the length of the branch and the separation between branches on the backbone. Then there is the number of branches per backbone. One can also have branches on the branches. Moreover, all of these variables will have some distribution in values, which may or may not be

* Corresponding author.
† Current address: Department of Chemical Engineering, Cornell University, Ithaca, NY 14853.
‡ Current address: 16503 Scenic Peaks Ct., Houston, TX 77059-5554.

10.1021/ma0117559 CCC: $22.00
Published on Web 03/09/2002

correlated with each other. Thus, the precise description of the LCB in a particular sample is highly complicated.

It is therefore critical to the development of an understanding of LCB to study polymers with simple, well-characterized LCB so that the basic rules of their behavior can be established. To date, this has been done primarily on anionically polymerized materials, both for the ability to make polymers that are nearly monodisperse and also for the availability of various coupling techniques to control the architecture of the polymers made.[12] Much of this sort of work has been done on symmetric stars (i.e., equal arm lengths) made from several different monomers.[13,14] For example, stars with various length arms have become available due to the miktoarm techniques of Hadjichristidis et al.[15,16] There has also been some work on anionically produced polymers with multiple branch points, including some comb polystyrenes[17] and pom-pom polyisoprenes.[18]

Our aim in this study was to investigate a series of polymers which all have the architecture of PE on the monomer scale but which vary widely in the nature of their long branches. The synthesis and characterization of these polymers has been described in an earlier paper.[19] All of them have a local structure identical to an LLDPE with 7−10 wt % butene (i.e., two to three ethyl branches per 100 backbone carbons). In this paper, the samples are named by type ("PEL" for linear, "PES" for star, "PEC" for comb, etc.) with numbers representing the number-average molecular weight of the polybutadiene precursors. See the tables or the previous paper[19] for details. The type of polymers we have made and examined include those with no long branches (linears); those with a single branch, where the length and position of the branch can be independently varied (stars); those with multiple branches, with a precise control of both the length and number of branches (pom-poms); and those with many branches of a fixed length, but where the number of LCB per chain is randomly distributed (combs). In this paper, we show how the melt rheology of PE depends on the nature of the branching over a broad range of variables.

Experimental Section

Synthesis and Characterization of Polymers. The general scheme to produce these model polyethylenes was to use various anionic techniques to make polybutadienes (PBds) in a linear, star, comb, or pom-pom architecture, followed by catalytic saturation.[20] To be sure that the model LCB PEs had the structures we were seeking to investigate, it was critical to have them well characterized at every stage of synthesis for molecular weight, saturation, and architecture. The methods used for the synthesis and characterization of all of these model PEs used herein were given in a recent paper[19] and the results for these polymers can be found in Tables 1−4.

Melt Shear Rheological Measurements. All samples were stabilized by dry blending the polymer sample with 1 wt % of a 1:2 mix of hindered phenol (Irganox 1076) and phosphite (Irgafos 168) stabilizers followed by compression molding to incorporate the stabilizer and to create the test specimens. Rheological testing was performed on a Rheometrics Scientific RMS-800 mechanical spectrometer that was equipped with 25 mm diameter parallel plates. In all cases the amount of polymer available for testing was quite limited, in some cases as low as 1.5−2 g. Consequently, a method was developed to perform small amplitude oscillatory shear measurements on a single specimen, or at most two to three specimens, at an extended series of temperatures. Application of this method required maintaining a constant gap between the plates (sample thickness) by compensating for tooling expansion/contraction with changes in the test.

The strain that was applied to each specimen during testing was chosen to ensure that the obtained data resided in the linear viscoelastic regime. The range of temperature probed was from 120 or 130 °C to 280 or 300 °C, and frequency was varied from 0.1 or 0.01 rad/s to 100 rad/s. These ranges were chosen to attempt to cover both the terminal (low frequency, high temperature) and plateau modulus (high frequency, low temperature) regions. Unfortunately, it was not always possible to access both regimes. We also needed to ensure that no significant degradation of the samples occurred at high temperature. The initial test was always performed at 150 °C, and after testing at the highest temperature for a particular specimen the sample was returned to 150 °C for a repeat test. In general, very good agreement between 150 °C runs was observed. Whenever serious discrepancies were observed, the highest temperature results were discarded. In early experiments, SEC measurement of MWD on "before" and "after" (after the entire residence time−temperature history through 280 °C testing) showed excellent agreement, which confirmed the rerun test at 150 °C.

For each sample, data at the various temperatures were superposed to a reference temperature of 190 °C by combined vertical and horizontal shifting of the log G^* vs log ω curves (where G^* is the complex modulus and ω is frequency). This superposition was performed in all cases using the commercial software package IRIS (Innovative Rheological Interface Software).[21] The vertical shifting to the reference temperature was performed first, with shift factors defined by

$$b_T = \rho_0 T_0/\rho T \tag{1}$$

where ρ is density, T is absolute temperature, and the subscript, "0", refers in all further discussion to the reference temperature of 190 °C. Following the vertical shifting arbitrary horizontal shifting was carried out until the best superposition of G^*, particularly in the terminal zone, was obtained by inspection. The latter shifting yielded the final master curve and the horizontal shift factors, a_T. Because the temperatures that were probed exceeded the glass temperature of PE by more than 100 K, the temperature dependence of a_T may be expected to follow an Arrhenius (Andrade) equation. Thus,

$$a_T = B \exp(E_a/RT) = \exp\{(E_a/R)(1/T - 1/T_0)\} \tag{2}$$

where T is the absolute temperature and E_a, the energy of activation for flow.

Extensional Rheology. Transient uniaxial extensional viscosity of the molten polymers was measured using the Rheometrics Scientific melt elongational rheometer (RME). The RME applies uniaxial extensional deformation to a molten rectangular parallelepiped polymer sample at a constant differential rate of strain via two pairs of rotating clamps that are imbedded in a temperature-controlled oven. The molten sample is supported over a brass air table via the flow of heated (to the desired test temperature) nitrogen gas through a porous brass frit that is positioned below the specimen. The transient extensional viscosity is then determined by measuring the resistant force that the polymer melt imparts on one pair of the rotating clamps during the application of the deformation and the prescribed strain rate. A leaf-spring type transducer, whose applicable range is 0.001−2.0 N, measures the former. Additional details of this instrument are available in the research literature.[22]

The samples in this work were prepared by compression molding rectangular parallelepipeds whose length, width and thickness were approximately 60, 8, and 1.5 mm, respectively. Prior to molding of the polymer, it was stabilized by adding 1 wt % Irgafos 168 to the granules. All tests were conducted at 150 °C. During testing, the deformation of each sample was observed using a CCD camera and monitor to ensure that the melt deformed homogeneously along its length. When nonuniform deformation occurred, the acquired data was discarded, a second test specimen was prepared, and the experiment was repeated.

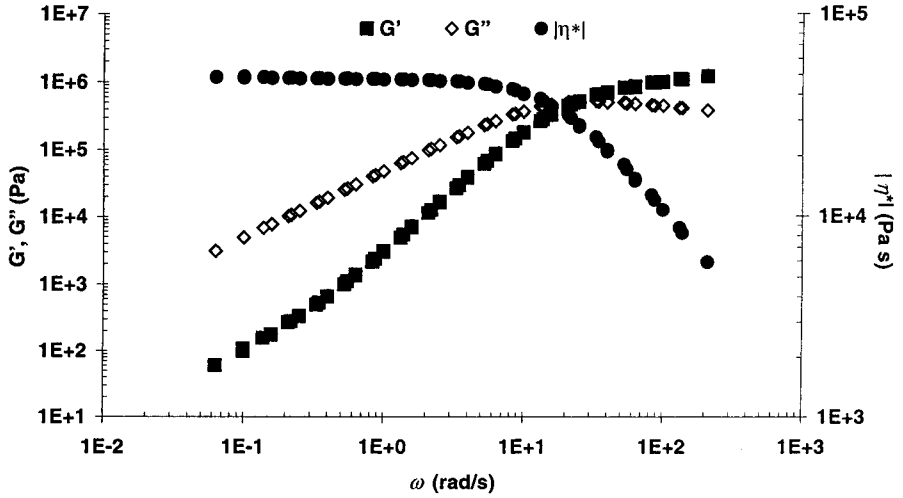

Figure 1. G', G'', and $|\eta^*|$ of PEL243 vs ω. Reference temperature is 190 °C.

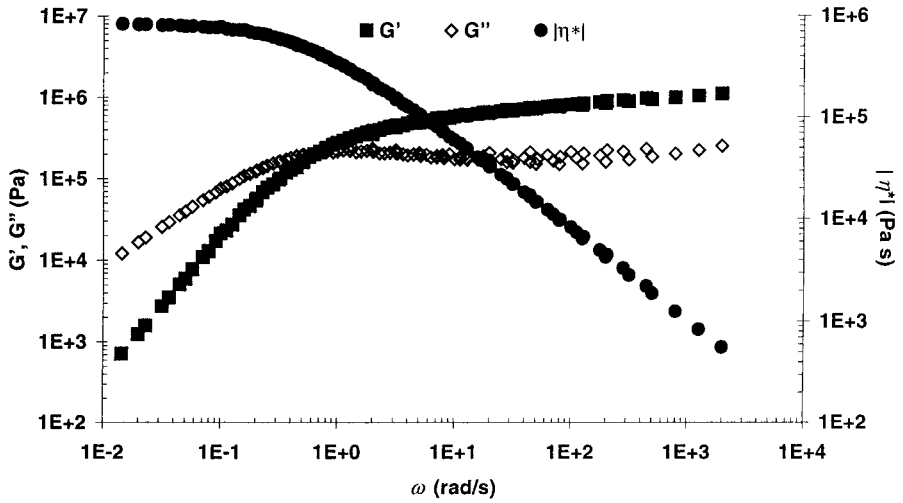

Figure 2. G', G'', and $|\eta^*|$ of PES(50)$_2$(5) vs ω. Reference temperature is 190 °C.

Analysis of Shear Results

The rheological results for the groups of essentially monodisperse model polymers studied here are divided into the following classifications: (a) linear, (b) symmetric three-arm stars (including blends with linear polymer), (c) asymmetric three-arm stars, (d) combs (randomly placed equal length branches), and (e) H−'s and a pom-pom. Figure 1 shows a typical set of log−log master curve plots of G' (storage, or elastic modulus), G'' (loss modulus), and $|\eta^*|$ (magnitude of complex viscosity) vs frequency for the 190 °C reference temperature for a linear (PEL243), and Figure 2 shows those for a star-branched polymer (PES(49)$_2$(5)), respectively. Generally, the results for the various samples comparing the differing structures are given in terms of the $|\eta^*|$ (190 °C) master curves for simplicity.

Figures 1 and 2, in addition to showing melt viscoelastic behavior typical of all of the model polymers, illustrate an observation concerning the time−temperature superposition. Excellent superposition of both G' and G'' was observed in essentially all linear polymer cases, while for the LCB containing cases good superposition of G' was generally obtained, but dispersion (lack of superposition) was observed for G'' in the plateau region. Moreover, the lack of superposability appears greater as the length and number of branches increases. Thus, our results support the hypothesis of thermorheological simplicity for linear polymer and thermorheological complexity for LCB polymers. However, additionally, we observe varying degrees of thermorheological complexity depending on the nature of the LCB architecture.

The limiting "zero shear" viscosity, η_0, was calculated from the Cross three-parameter fitting equation[23]

$$\eta^*(\omega) = \eta_0/[1 + (\lambda\omega)^{1-a}] \tag{3}$$

(where λ is a characteristic relaxation time and a is the power law exponent when the data extend into the terminal region). In general, this agreed well with the observed Newtonian behavior at low frequencies. Additional rheological parameters, which are included in the appropriate tables, are E_a, defined in eq 2, λ, defined in eq 3, the steady-state compliance, J_e^0, the rubbery plateau modulus, G_N^0, and the entanglement molecular weight, M_e. Here, J_e^0 and M_e are calculated, respectively by

$$J_e^0 = (1/\eta_0^2)\lim_{\omega\to 0}(G'/\omega^2) \tag{4}$$

and

$$M_e = \rho RT/G_N^0 \tag{5}$$

Table 1. Model Linear E−B Copolymer Molecular/Rheological Parameters (T_{ref} = 190 °C)

sample	butene content (wt %)	M_w (kg/mol)	η_0 (Pa s)	λ (s)	E_a (kJ/mol)	J_e^0 (MPa^{-1})	G_N^0 (MPa)	M_e (kg/mol)
PEL19	8.6	19.3	1.03×10^1		32.2	0.94		
PEL90	6.4	90.2	2.24×10^3	9.1×10^{-4}	30.5	0.87		
PEL1234	7.8	124	6.89×10^3	3.9×10^{-3}	29.7	0.99		
PEL125	7.9	127	6.58×10^3	3.7×10^{-3}	28.0	1.1	2.45	1.19
PEL147	7.5	148	1.01×10^4	4.9×10^{-3}	28.9	0.95	1.97	1.48
PEL193	7.5	195	2.85×10^4	1.3×10^{-2}	29.7	0.81	1.79	1.63
PEL243	8.1	255	4.93×10^4	3.0×10^{-2}	29.3	1.1	1.75	1.67
PEL280	7.3	290	9.22×10^4	5.7×10^{-2}	(24.7)		1.86	1.57
PEL685	7.3	789			29.7		2.00	1.46

where $\rho = 758$ kg/m^3 at 190 °C and R is the gas constant (8.314 J/K/mol). The values of G_N^0 were obtained by the integration of the G'' data as follows:

$$G_N^0 = \frac{2}{\pi}\int_{-\infty}^{+\infty} G''(\omega)\, \mathrm{d}(\ln \omega) \qquad (6)$$

Since we were unable to access the very high-frequency region, to perform this integration we had to extrapolate the G'' data to calculate G_N^0. In a number of cases, either the terminal region or the plateau region could not be accessed, so the associated parameters are not reported. Additionally, at low frequencies and low instrument torques, G' sometimes showed severe noise and/or a systematic error (concave upward curvature, rather than linear log−log behavior with a slope of two) preventing determination of J_e^0. However, even in the presence of these low-frequency problems, terminal regions where $\mathrm{d}(\log G')/\mathrm{d}(\log \omega) = 2$ and $\mathrm{d}(\log G'')/\mathrm{d}(\log \omega) = 1$ are observed at higher frequencies (see Figures 1 and 2), thus permitting evaluation of the terminal region parameters.

Discussion of Shear Results

Linear Polymers. In all, nine linear samples were studied, ranging in M_w from 19 to 780 kg/mol. The only relevant structural parameters are M_w and short chain branching (labeled in the tables as "butene content" because these polymers have the structure of ethylene−butene copolymers) since $M_w/M_n < 1.1$ in all cases. Table 1 gives the structural and rheological parameters noted above. In these cases, most of the accessed data are in the Newtonian (terminal) region, but where shear thinning is observed, convergence to a single high-frequency behavior is seen. The data in Table 1 also show that both the flow activation energy, E_a, and plateau modulus, G_N^0, are independent of molecular weight for these linear polymers. The average value of G_N^0 for these linear polymers is 1.97 MPa, which is close to the literature values.[2]

An important check of the validity of the general methods used in this work is to compare the η_0-M_w relationship obtained here to those found in the literature. From the data in Table 1 we have

$$\log \eta_0(190\ °C) = -13.219 + 3.33(\log M_w) \qquad (R = 0.9987) \quad (7)$$

or

$$\eta_0(190\ °C) = 6.04 \times 10^{-14} M_w^{3.33} \qquad (8)$$

with the exponent close to the expected value of 3.4. This is very similar to the results of Mendelson et al.[1] and of Raju et al.[24−28] This excellent agreement is clear in Figure 3, which combines results on linear hydrogenated polybutadienes from this work with those of Raju et al.

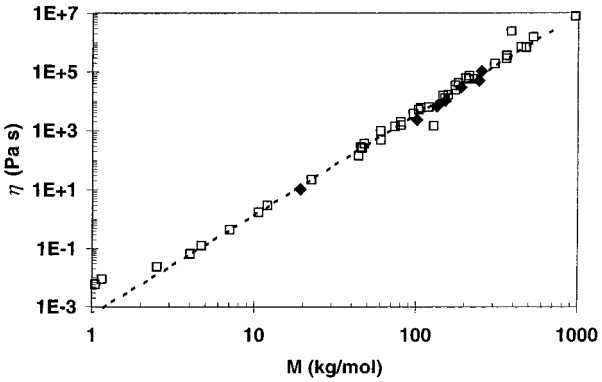

Figure 3. Dependence of η_0 on molecular weight for linear polymers. Data were taken from this work (filled diamonds) and refs 24−28 (open squares).

Stars. In this work we are interested in studying the effects of branch length and the number of branches per backbone on rheological behavior, rather than a more general investigation of the properties of star polymers. So we have concentrated on branched polymers with backbones of close to 100 kg/mol, and only a few symmetric three-arm stars were examined. In this paper, we define the backbone of star polymers to be the sum of the lengths of the longest two arms. As can be seen from the results presented in Table 2, star polymers tend to have much longer relaxation times than linear polymers of similar molecular weight, as well as much higher values of η_0 and E_a.

It has long been observed that η_0 for symmetric stars does not depend on the total molecular weight, nor on the functionality of the stars, but rather exponentially on the arm molecular weight, M_{arm}.[29] This is in marked contrast to the power-law dependence on molecular weight seen for linear polymers (viz. Figure 3). This occurs because the stress relaxation of stars is controlled by arm retraction, rather than chain reptation, as in the case of linear polymers. One equation which has been put forth for the M_{arm} dependence of η_0 in stars is

$$\eta_0 = A \exp\left\{\gamma \frac{M_{arm}}{M_e}\right\} \qquad (9)$$

where γ and A are constants independent of M_{arm}. It has generally been found that $\gamma \cong 0.6$.

The values for the two symmetric stars in Table 2 agree well with those from Raju et al.[24−28] We are interested to see if the value of M_e extracted from these data agrees with that derived from the plateau moduli

Table 2. Model Three-Arm Star E−B Copolymer Molecular/Rheological Parameters (T_{ref} = 190 °C)

sample	butene content (wt %)	M_w[a] (kg/mol)	M_{arm}[b] (kg/mol) A	B	η_0 (Pa s)	λ (s)	E_a (kJ/mol)	J_e^0 (MPa^{1-})	G_N^0 (MPa)	M_e (kg/mol)
symmetric stars										
$PES(43)_3$	9.0	133	43		5.7×10^6	3.71×10^1	71.1	~14		
$PES(48)_3$	6.8	***133***	48		*d*	*d*	d	d	d	d
$PES(50)_3$	8.7	194	50		3.5×10^8	2.36×10^3	75.7	~29		
asymmetric stars										
$PES(50)_2(5)$	8.9	130	50	5	9.25×10^5	1.83×10^0	59.8		0.975	2.99
$PES(49)_2(5)$	11	105	49	5	2.99×10^5	1.19×10^0	59.4			
$PES(50)_2(15)$	7.9	138	50	15	8.56×10^6	9.89×10^1	54.8	17.5		
$PES(50)_2(25)$	7.5	131	50	25	2.28×10^6	3.09×10^1	68.2	26		
$PES(15)_2(85)$	9.9	129	15	85	4.6×10^7	3.86×10^2	66.1	13		
$PES(40)_2(60)$	9.0	132	40	60	6.42×10^6	6.23×10^1	70.3	24.1		
linear/star blends										
PELS(95H/5L)	7.5	[c]147	48		1.29×10^4	8.29×10^{-3}	29.3	15.5		
PELS(90H)(10L)	7.4	[c]147	48		1.70×10^4	1.52×10^{-2}	30.1	16.8		
PELS(50H)(50L)	7.1	[c]141	48		2.17×10^5	4.27×10^0	42.7	30.9		

[a] Total $\bar{M}_w$ measured by GPC-MALLS on hydrogenated samples. [b] Arm $\bar{M}_n$ determined on polybutadiene precursors. [c] Calculated from components. [d] Not measured, used in blends.

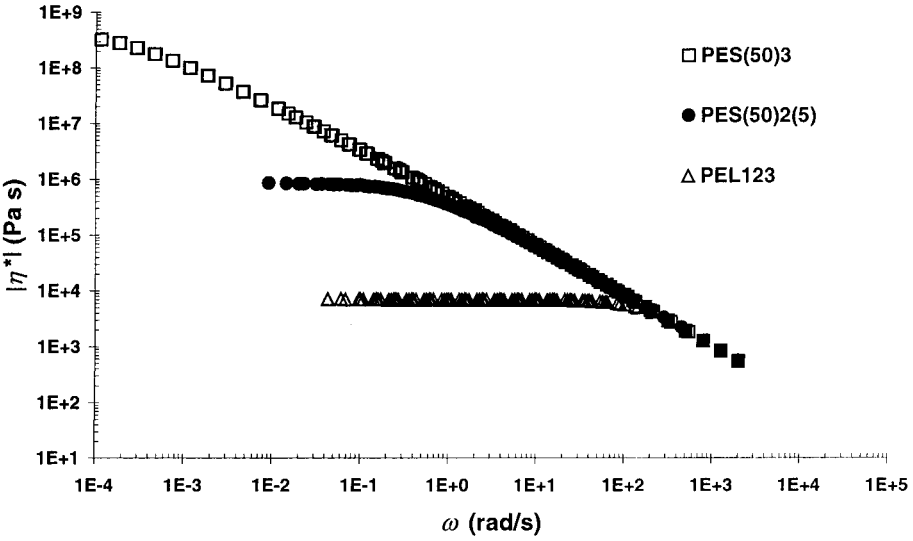

Figure 4. $|\eta^*|$ for stars.

of the linear polymers. Fitting the combination of the Raju data and those reported herein to eq 9 yields

$$\eta_0 = 6.96 \exp\{2.63 \times 10^{-4} M_{arm}\} \qquad (10)$$

which, taking $\gamma = 0.6$, gives $M_e = 2.28$ kg/mol. This result is intermediate between the values of M_e and M_c for polyethylene,[2] which suggests a deficiency in the current models of arm retraction.[30]

Many more asymmetric stars were examined, made by the miktoarm synthesis scheme outlined in the first paper of this series.[15] Again, these polymers were made so that the effective backbone (that is, the sum of the lengths of the two longest arms) was close to 100 kg/mol. The "branch" (the shortest arm) varied from 5 to 50 kg/mol. In most cases, this was placed in the center of the backbone, but in several cases, it was placed off-center by having unequal lengths for the two longer arms of the star. Again, these asymmetric stars showed much higher values of λ, η_0, and E_a in comparison to the linear polymers, as seen in Table 2. Even a very short branch of 5 kg/mol (only a few times M_e) is sufficient to show the effect, which is due to the great increase in relaxation times that arise from the need to retract an entangled branch in order for the backbone to relax. Figure 4 shows how η_0 increases monotonically as the length of the central branch rises. No simple formulas, like those of eqs 9 and 10, have yet been found to describe the viscosities of asymmetric stars.

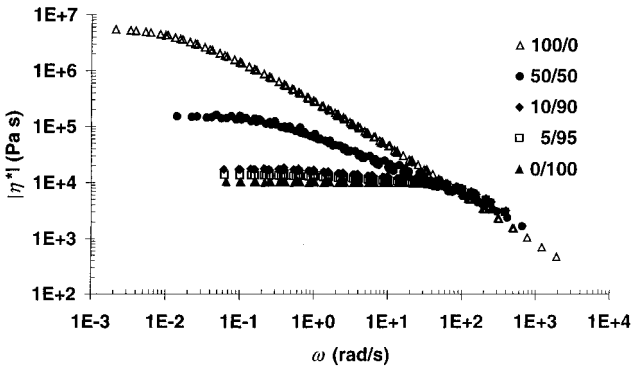

Figure 5. $|\eta^*|$ for star−linear blends.

Figure 5 shows the linear/star blends (PELS(95H)-(5L), PELS(90H)(10L), and PELS(50H)(50L)) along with those for the two components (linear PEL148 and star-branched $PES(43)_3$). The progression of low frequency viscosity magnitude follows nicely with concentration

Table 3. Model Comb and α−ω Polymerized Copolymers: Molecular Structure

sample	butene content (wt %)	M_w[a] (kg/mol)	M_{bb}[b] (kg/mol)	M_{conn}[b] (kg/mol)	M_{arm}[b] (kg/mol)	n_{arm}[c]
combs						
PEC(101)-*g*-(7)$_{30}$	9	426	103		6.5	30
PEC(97)-*g*-(23)$_{26}$	10	735	97.0		23.5	26
PEC(100)-*g*-(5)$_2$	9	105	90.0		4.5	2
PEC(100)-*g*-(5)$_{12}$	10	171	99.7		5.3	12
PEC(108)-*g*-(6)$_{12}$	9	170	109		5.8	12
α−ω type polymers (H−/pom-pom)						
PEH(6)$_2$(27)(6)$_2$	10	46.6		24.9	6.2	4
PEH(12)$_2$(27)(12)$_2$	10	64.7		24.9	10.8	4
PEPP(10)$_5$(92)(10)$_5$	10	247		109	10.5	10

[a] Total $\bar{M}_w$ measured by GPC-MALLS on hydrogenated samples. [b] Backbone, connector, and arm $\bar{M}_n$ determined on polybutadiene precursors. [c] Average number of arms determined by ^{13}C NMR.

Table 4. Model Comb and α−ω Polymerized Copolymers: Rheological Parameters (T_{ref} = 190 °C)

sample	M_w (kg/mol)	η_0 (Pa s)	λ (s)	E_a (kJ/mol)	J_e^0 (MPa^{-1})	M_e (kg/mol)	G_N^0(measd) (MPa)	G_N^0(calcd)[c] (MPa)
combs								
PEC(101)-*g*-(7)$_{30}$	426	1.07×10^6	1.64×10^1	77.0		12.2	0.240[b]	0.208
PEC(97)-*g*-(23)$_{26}$	735	$>5 \times 10^7$ [a]	- N/A-	73.6		117.	0.025[b]	0.038
PEC(100)-*g*-(5)$_2$	105	7.48×10^3	2.36×10^{-2}	34.9		2.23	1.31[b]	1.63
PEC(100)-*g*-(5)$_{12}$	171	4.74×10^6	1.57×10^1	74.9		3.80	0.768[b]	0.770
PEC(108)-*g*-(6)$_{12}$	170	N/A[a]	N/A	71.1		3.26	0.894[b]	0.709
α−ω type polymers (H−/pom-pom)								
PEH(6)$_2$(27)(6)$_2$	46.6	6.43×10^3	1.44×10^{-2}	51.0		4.36	0.669[b]	0.552
PEH(12)$_2$(27)(12)$_2$	64.7	7.13×10^4	5.30×10^{-1}	66.1		7.08	0.412[b]	0.255
PEPP(10)$_5$(92)(10)$_5$	247	N/A[a]	N/A	57.3				0.452

[a] Terminal region not accessed, PEC(97)-*g*-(23)$_{26}$ close. [b] Obtained from eq 6; in most cases, this is a secondary, apparent plateau. [c] Calculation of apparent plateau modulus obtained from eq 11, assuming backbone is diluted by the arms and α = 2.0.

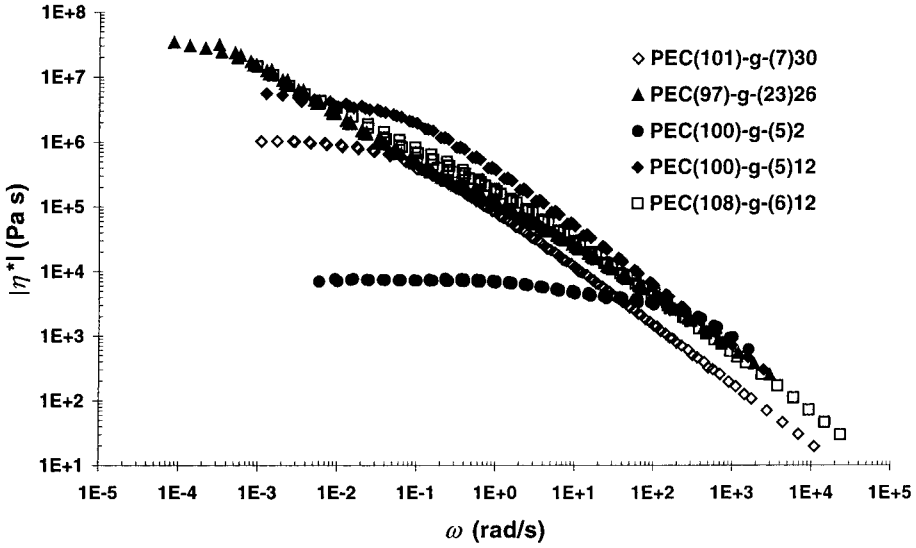

Figure 6. |η*| for combs.

of branched polymer present, and in these graphical representations, the enhancement of low frequency (low shear) viscosity by orders of magnitude due to branching is apparent. More work on blends of these models will be done in the near future.

Comb and α−ω (H−/Pom-Pom) E−B Polymers. The comb structures and the α−ω polymer structures investigated encompass a larger group of architectural parameters, as shown in Table 3. Again, for this study, we limited the immense range of possible architectures by looking at polymer with $M_{backbone} \approx 100$ kg/mol. It should be noted that in the combs the arms are randomly distributed (but all arms in a sample are equal length). Only a few of the α-ω polymers (pom-poms and H's) were examined, and in these the placement of the branches is more precise than in the combs. These structural features again create multiple orders of magnitude differences in low-frequency viscoelastic behavior, but also have significant effects on the apparent plateau modulus, G_N^0, and the shear thinning characteristic of the viscosity, which is listed in Table 4.

Figure 6 shows a comparison of the |η*| curves for the five investigated combs, and Figure 7 similarly compares G' curves among these samples. These figures show that the great variety of structures leads to a wide variety of rheological behavior. The zero-shear viscosity, for instance, is not simply dependent on the degree of branching. In Figure 8, we compare the G' and viscosity curves of PEL243, PES(50)$_2$(5), and PEC(101)-*g*-(7)$_{30}$.

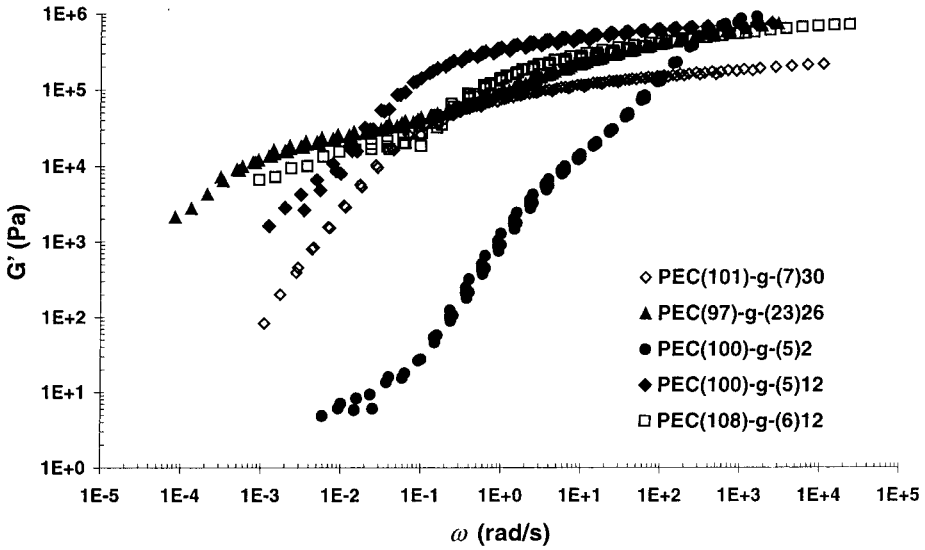

Figure 7. G′ for combs.

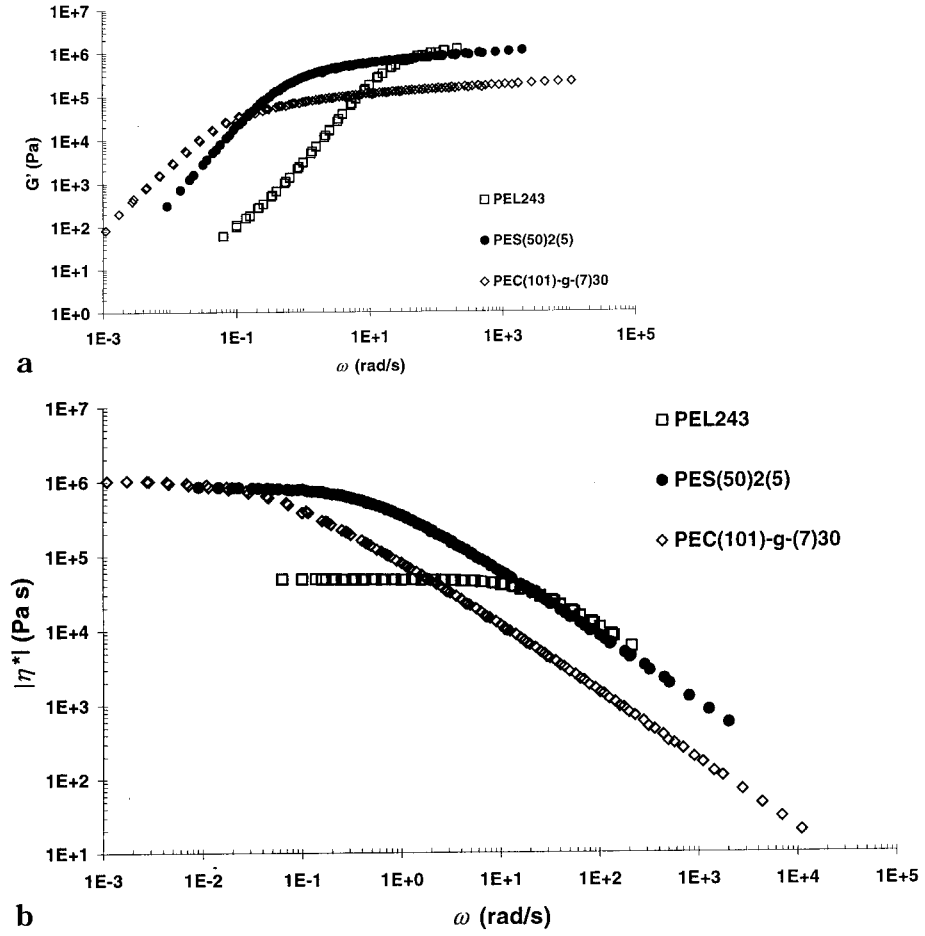

Figure 8. (a) G' for PEL243, PES$(50)_2(5)$, and PEC(101)-g-$(7)_{30}$. (b) $|\eta^*|$ for PEL243, PES$(50)_2(5)$, and PEC(101)-g-$(7)_{30}$.

The single, short branch of PES$(50)_2(5)$ is enough to greatly enhance η_0 over that of PEL243, but the comb with 30 branches of about the same length as the one of the star has about the same η_0. There is a balance between the slowing down of the polymer due to branching and the drop in their chain size, also due to the branches.

In general, the way that η_0 depends on the structure of multibranched polymers is quite complicated. Figure 9 shows η_0 for all of the polymers in this study, as well as those of similar chemical type in the literature.[24−28] It is not clear that any simple relation can be found that covers all of these cases. This means that a measure of η_0 alone cannot be used as a measure of LCB. The case is similar for the flow activation energy. Figure 10 shows E_a for the same set of polymers. While E_a is certainly larger for the branched polymers than for the linears, there is no obvious pattern that can be used to specify the nature of the LCB from just a knowledge of E_a alone. The application of melt rheology as a tool to characterize

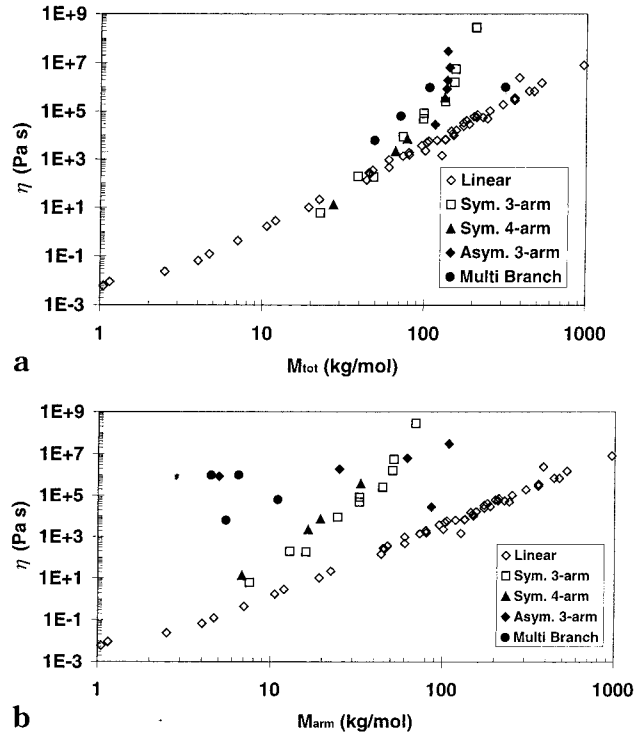

Figure 9. (a) η_0 vs M_{tot} (i.e., the M_w of the whole molecule) for all polymers. (b) η_0 vs M_{arm} for all polymers.

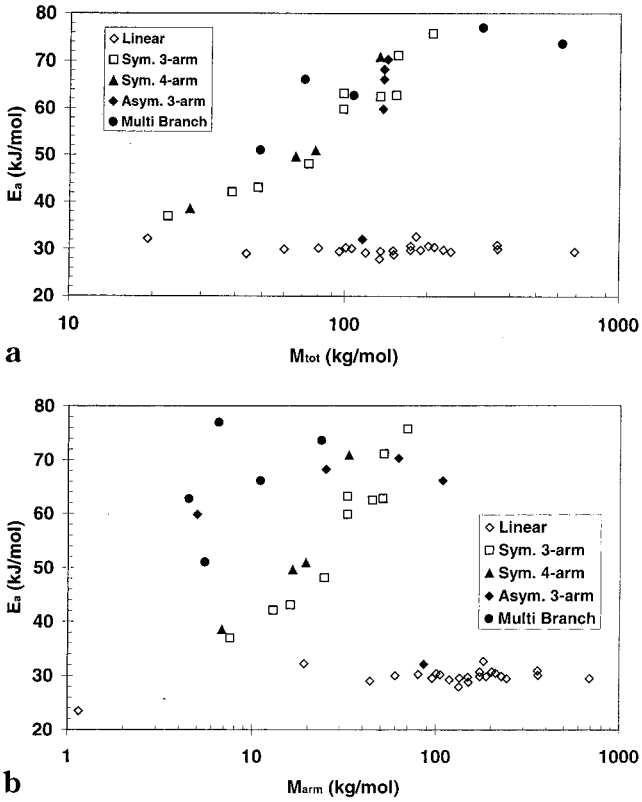

Figure 10. (a) E_a vs M_{tot} (i.e., the M_w of the whole molecule) for all polymers. (b) E_a vs M_{arm} for all polymers.

the type and degree of LCB requires a more detailed analysis of the data.

An example of this can be seen in the elastic modulus of PEC(101)-*g*-$(7)_{30}$, which is presented in Figure 11. This modulus plateaus at a value that is approximately 0.240 MPa, which is well below the G_N^0 value reported for the linear polymers (1.97 MPa). Does this apparently much lower value of G_N^0 mean that the comb is much less entangled than a linear equivalent? The situation becomes clearer by comparing this with the behavior of PEC(97)-*g*-$(23)_{26}$. This comb not only shows a low apparent plateau but also the normal plateau of the linear polymers. This behavior was first seen in polystyrene combs by Roovers and Graessley.[17] The secondary apparent plateau modulus arises due to the great separation of relaxation times that arises in comb polymers. In this frequency region, the branches have completely relaxed, but they still act to hold the backbone. The value of the apparent plateau can be calculated by assuming that the arms act simply as a diluent for the backbones. We can estimate this apparent plateau from the following equation

$$G_N^0(\phi) = G_N^0(\phi = 1)\phi^{\alpha} \qquad (11)$$

where α has a value between 2.22[27] and 2.0.[31] From Table 4 it can be seen that using a value of 1.97 MPa for $G_N^0(\phi = 1)$ (the plateau modulus for linear polymers of this chemistry, as seen in Table 1) and $\alpha = 2.0$ gives quite a reasonable agreement with what has been measured for these combs. Similar behavior is also found for the α−ω polymers. The level of this apparent plateau may, therefore, be used to characterize the amount of branches in a sample, and the frequency range over which it appears may tell us how long the branches are. This is pursued further in the next section, in which we use a new method to analyze the shear data.

Van Gurp−Palmen Analysis. A new way to look at the data obtained from small amplitude oscillatory shear experiments has recently been proposed.[32] By using this technique on the model polymers with well-defined branching that we are discussing here, we hope to make this a quantitative way to extract more information on the nature of LCB in a sample.

The main idea of the so-called Van Gurp−Palmen analysis is to plot δ (=$\tan^{-1}[G''/G']$) vs the magnitude of the complex modulus, $|G^*|$. Figure 12 shows this sort of plot for all of the linear polymers in this study. All of the data fall on one curve, with a very characteristic shape. At low values of $|G^*|$ δ is nearly 90°, meaning that the samples are nearly totally viscous. The point at which the value drops precipitously to 0° (corresponding to complete elastic behavior) is close to the plateau modulus. The behavior of the stars is quite different from that of the linear polymers (Figure 13), and the difference in the area under the curves can be related to the degree of branching.[33] More intriguing are the Van Gurp−Palmen curves of the combs (Figure 14). Note that the minimum in δ at 0.160 MPa is again close to the value of the apparent plateau for PEC(101)-*g*-$(7)_{30}$, which is 0.240 MPa. This is also seen for PEC-(108)-*g*-$(6)_{12}$, with the hint of a minimum just below the apparent plateau of 0.894 MPa. This can be used to estimate the "secondary" plateau modulus for PEC(97)-*g*-$(23)_{26}$, which could not be calculated from the integration of the G'' data by eq 6. For this comb there is a minimum in δ at 0.029 MPa, so we can project an apparent plateau of about 0.035 MPa. The prediction of eq 11 from arm dilution for PEC(97)-*g*-$(23)_{26}$ is 0.019 MPa, which is relatively low as for the other combs. This comb also shows the approach to the true plateau, as can be seen in Figure 14. The depth of the drop at the

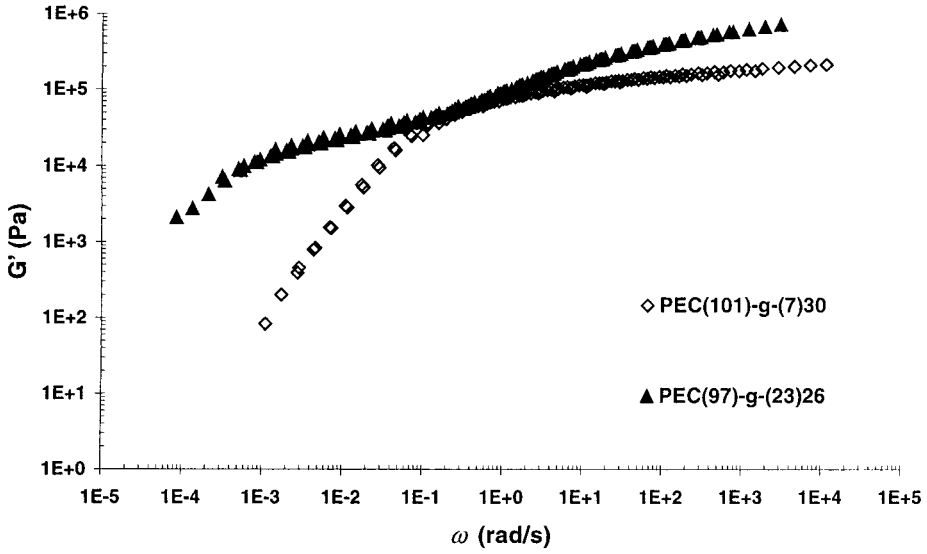

Figure 11. G' for PEC(101)-g-(7)$_{30}$ and PEC (97)-g-(23)$_{26}$.

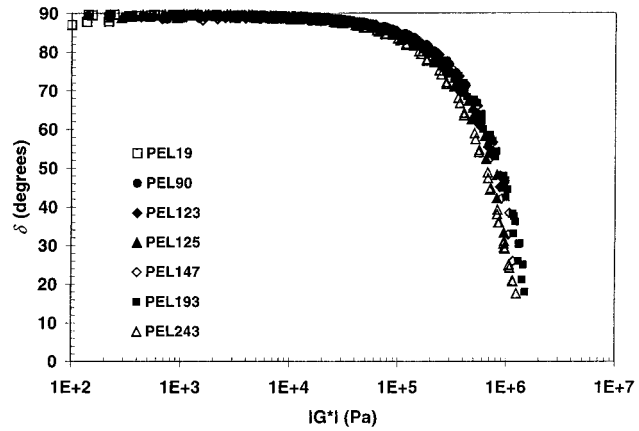

Figure 12. Van Gurp−Palmen plot for linear polymers.

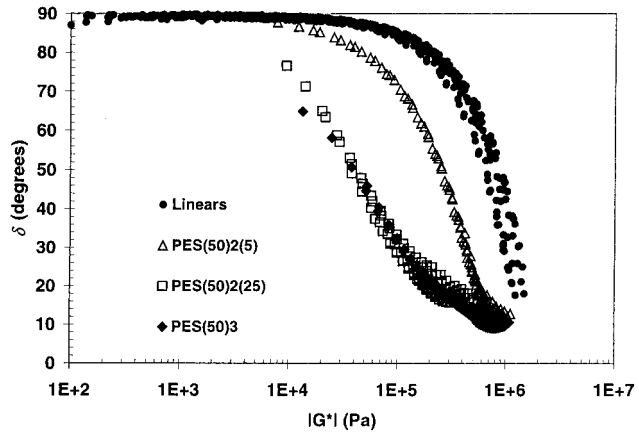

Figure 13. Van Gurp−Palmen plot for star polymers.

apparent plateau may also be related to the lengths of the arms, relative to that of the backbone. Obviously, there are no more data in the Van Gurp−Palmen curve than in the usual curves of G' and G'' vs ω, but this form of presentation shows the LCB features more transparently and serves as a useful tool for the rheological characterization of LCB.

Discussion of Extensional Results

We have obtained extensional data on only a few of these samples, due to the difficulties in running this

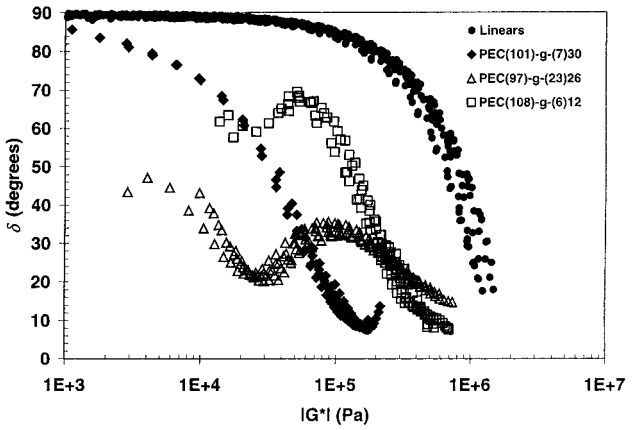

Figure 14. Van Gurp−Palmen plot for comb polymers.

experiment. However, the results that have been obtained also shed a great deal of light on the nature of LCB in these polymers. In combination with shear and light-scattering analysis, they hold the promise of providing extensive characterization of the LCB for an unknown sample.

Although all kinds of LCB will enhance the shear thinning of a polymer, as seen above, it has been posited that only polymers with multiple long branches per chain will exhibit thickening in extension.[33] We have tested this by looking at linear polymers and several blends of linear and model LCB polymers. (It has proved impossible to measure the extensional rheology of the pure combs, due to their high elasticity. The linear polymer used here was an ethylene−hexene copolymer, Exceed 1018, a linear low-density polyethylene from ExxonMobil Chemical Co. with a melt index of 1 g/10 min and a density of 0.918 g/cm^3.) The Meissner RME instrument gives data on the transient extensional viscosity as a function of time. From the shear rheology and the assumption of linear viscoelasticity, one can predict what the extensional behavior in the limit of small strains, which serves as a baseline for determining the behavior of the polymer to uniaxial extensional deformation. If the measured extensional viscosity is substantially above the linear viscoelastic limit, then it is said to display extensional thickening.

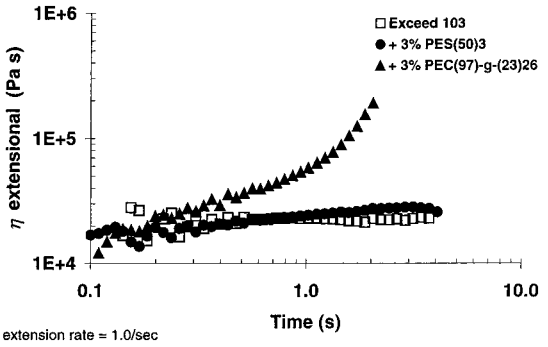

Figure 15. η_{ext} for Exceed 1018 and blends with star and comb polymers.

As seen in Figure 15, both the pure linear polymer and its blend with 3% of PES$(50)_3$ show similar behaviors. The extensional viscosity was exactly that predicted by linear viscoelasticity from the shear data, so neither sample showed extensional thickening. However, when 3% of PEC(97)-*g*-$(23)_{26}$ was added to the linear polymer, a dramatic rise in η_{ext} was seen, indicating extensional thickening. That this can be seen with such a small addition of comb is remarkable. Future work will be aimed at understanding what levels of comb are needed to show this behavior, and how it can be related to the melt strength of the polymers.

Conclusions

A set of polymers with a broad range of LCB architecture has been made with the monomeric-scale structure of LLDPE. These have allowed us not only to establish ways by which to characterize the structure of LCB in PE materials but also to determine how the rheology of such polymers depends on the form of the LCB. The main results of this rheological analysis can be briefly stated as follows:

•All polymers that have LCB show a greater degree of shear thinning than linear chains. This applies both to those with a single branch (stars) and also to those with multiple branches per chain (combs, H-type). The results presented in this paper show how the degree of shear thinning depends on the detailed nature of the LCB.

•Only molecules with multiple branches induce extensional thickening in a sample, not linear or star chains. Only a small amount of these comblike molecules, on the order of 5%, are needed to show this effect.

•The melt rheology of these polymers is the most sensitive characterization tool for LCB type and level. From the points made above, it is clear that measuring both the shear and extensional rheology can help distinguish the presence of any branches, and can also determine the presence and level of combs that are present. We also show here how a new method of treating the shear data, the so-called Van Gurp−Palmen analysis, can give a more easily interpreted form of the results that can reveal the length and amount of branches in a sample.

While all of these data have been obtained on polymers with the local monomeric structure of LLDPE, these results apply equally well to polyamides, polystyrene, or in fact to any flexible polymer. The insights generated from this work show the importance of access to well-defined polymers with several kinds of branching architecture for the development of a deeper understanding of polymer rheology.

References and Notes

(1) Mendelson, R. A.; Bowles, W. A.; Finger, F. L. *J. Polym. Sci., Part A-2* **1970**, *8*, 105.

(2) Fetters, L. J.; Lohse, D. J.; Colby, R. H. In *Physical Properties of Polymers Handbook*, Mark, J., Ed., AIP Press: New York, 1996. Fetters, L. J.; Lohse, D. J.; Milner, S. T.; Graessley, W. W. *Macromolecules* **1999**, *32*, 6847.

(3) Vega, J. F.; Muñoz-Escalona, A.; Santamaría, A.; Muñoz, M. E.; Lafuente, P. *Macromolecules* **1996**, *29*, 960.

(4) Malmberg, A.; Kokko, E.; Lehmus, P.; Löfgren, B.; Seppälä, J. V. *Macromolecules* **1998**, *31*, 8448.

(5) Quan, Z.; Cotts, P. M.; McCord, E. F.; McLain, S. J. *Science* **1999**, *283*, 2059.

(6) Cotts, P. M.; Quan, Z.; McCord, E. F.; McLain, S. J. *Macromolecules* **2000**, *33*, 6945.

(7) Helmstedt, M.; Stejskal, J.; Burchard, W. *Macromol. Symp.* **2000**, *162*, 63.

(8) Randall, J. C. *J. Macromol. Sci.—Rev.* **1989**, *C29*, 201.

(9) Vega, J. F.; Santamaría, A.; Muñoz-Escalona, A.; Lafuente, P. *Macromolecules* **1998**, *31*, 3639.

(10) Chai, C. K. *ANTEC Proc.* **2000**, 1096.

(11) Wood-Adams, P. M.; Dealy, J. M.; deGroot, A. W.; Redwine, O. D. *Macromolecules* **2000**, *33*, 7489.

(12) Krigas, T. M.; Carella, J. M.; Struglinski, M. J.; Crist, B.; Graessley, W. W.; Schilling, F. C. *J. Polym. Sci.—Phys.* **1985**, *23*, 509.

(13) Masuda, T.; Ohta, Y.; Onogi, S. *Macromolecules* **1971**, *4*, 763.

(14) Graessley, W. W.; Roovers, J. *Macromolecules* **1979**, *12*, 959.

(15) Iatrou, H.; Hadjichristidis, N. *Macromolecules* **1992**, *25*, 4649.

(16) Gell, C. B.; Graessley, W. W.; Efstratiadis, V.; Pitsikalis, M.; Hadjichristidis, N. *J. Polym. Sci., Part B: Polym. Phys.* **1997**, *35*, 1943.

(17) Roovers, J.; Graessley, W. W. *Macromolecules* **1981**, *14*, 766.

(18) McLeish, T. C. B.; Allgaier, J.; Bick, D. K.; Bishko, G.; Biswas, P.; Blackwell, R.; Blottière, B.; Clarke, N.; Gibbs, B.; Groves, D. J.; Hakiki, A.; Heenan, R. K.; Johnson, J. M.; Kant, R.; Read, D. J.; Young, R. N. *Macromolecules* **1999**, *32*, 6734.

(19) Hadjichristidis, N.; Xenidou, M.; Iatrou, H.; Pitsikalis, M.; Poulos, Y.; Avgeropoulos, A.; Sioula, S.; Paraskeva, S.; Velis, G.; Lohse, D. J.; Schulz, D. N.; Fetters, L. J.; Wright, P. J.; Mendelson, R. A.; García-Franco, C. A.; Sun, T.; Ruff, C. J. *Macromolecules* **2000**, *33*, 2424.

(20) Hadjichristidis, N.; Iatrou, H.; Pispas, S.; Pitsikalis, M. *J. Polym. Sci.—Chem.* **2000**, *38*, 3211.

(21) Winter, H. H.; Baumgartel, M.; Soskey, P. M. *Technol. Rheol. Meas.* **1993**, 123.

(22) Meissner, J.; Hostettler, J. *Rheol. Acta* **1994**, *33*, 1.

(23) Dealy, J. M.; Wissbrun, K. F. *Melt Rheology and Its Role in Plastics Processing—Theory and Applications*; Van Nostrand Reinhold: New York, 1990; p 162.

(24) Raju, V. R.; Rachapudy, H.; Graessley, W. W. *J. Polym. Sci.: Polym. Phys. Ed.* **1979**, *17*, 1223.

(25) Graessley, W. W.; Raju, V. R. *J. Polym. Sci.: Polym. Symp.* **1984**, *71*, 77.

(26) Raju, V. R. Rheological Properties of Linear and Star-Branched Hydrogenated Polybutadiene with Narrow Molecular Weight Distribution. Ph.D. Dissertation, Northwestern University, Evanston, IL, 1980.

(27) Raju, V. R.; Menezes, E. V.; Marin, G.; Graessley, W. W.; Fetters, L. J. *Macromolecules* **1981**, *14*, 1668.

(28) Pearson, D. S.; Fetters, L. J.; Graessley, W. W.; Ver Strate, G.; von Meerwall, E. *Macromolecules* **1994**, *27*, 711.

(29) Carella, J. M.; Gotro, J. T.; Graessley, W. W. *Macromolecules* **1986**, *19*, 659. Pearson, D. S. *Rubber Chem. Technol.* **1987**, *60*, 439.

(30) Levine, A. J.; Milner, S. T. *Macromolecules* **1998**, *31*, 8623.

(31) Tao, H.; Lodge, T. P.; von Meerwall, E. D. *Macromolecules* **2000**, *33*, 1747.

(32) Van Gurp, M.; Palmen, J. *Rheology Bull.* **1998**, *67*, 5. Trinkle, S.; Friedrich, C. *Rheol. Acta* **2001**, *40*, 322.

(33) McLeish, T. C. B.; Larson, R. G. *J. Rheol.* **1998**, *42*, 81.

MA0117559